

# Phenyl side group liquid crystal polymers

J. Liu and P. H. Geil\*

*Department of Materials Science and Engineering, University of Illinois at Urbana-Champaign, Urbana, IL 61801, USA*

and S.-M. Huh and J.-I. Jin

*Department of Chemistry, University of Korea, Seoul 136-701, Korea*

*(Received 30 August 1995; revised 19 October 1995)*

Poly(3-phenyl-4-oxybiphenylene-4'-carbonyl) (PPOBC) and poly(5-phenyl-2-oxy-6-naphthoyl) (PPONY) have been prepared as lamellar single crystals using the confined thin film melt polymerization technique. Electron diffraction indicates a monoclinic (pseudo-orthorhombic,  $\alpha = 90^\circ\text{C}$ ) cell with  $a = 15.24 \text{ \AA}$ ,  $b = 3.94 \text{ \AA}$  and  $c = 10.54 \text{ \AA}$  for PPOBC and an orthorhombic cell with  $a = 29.60 \text{ \AA}$ ,  $b = 5.08 \text{ \AA}$  and  $c = 16.74 \text{ \AA}$  for PPONY ( $1 \text{ \AA} = 0.1 \text{ nm}$ ). Modelling using the Cerius<sup>2</sup> program suggests a  $Pn11$  space group for PPOBC and a  $P2_1/c2_1/c2/n$  space group for PPONY. In contrast to the relatively low crystal–mesophase transition temperature ( $T_{k-m} = 350^\circ\text{C}$ ) for poly(phenyl-*p*-phenylene terephthalate), in which the phenyl rings would be expected to be randomly positioned on the *p*-phenylene residues, the regular conformations in these two polymers lead to high  $T_{k-m}$  ( $422^\circ\text{C}$  for PPOBC and  $528^\circ\text{C}$  for PPONY). Copyright © 1996 Elsevier Science Ltd.

**(Keywords: liquid crystal polymers; phenyl side groups; lamellar single crystals)**

## INTRODUCTION

The addition of phenyl side chains to main-chain aromatic thermotropic liquid crystal polymers might be expected to make crystal packing more difficult and thus lower the crystal–mesophase transition temperature ( $T_{k-m}$ ), permitting processing at lower temperature. For instance, considerable study has been made of polymers based on alternating ester groups and *p*-phenylene residues. The symmetric (alternating direction ester groups) poly(*p*-phenylene terephthalate) (PpPT) apparently has no  $T_{k-m}$ , Jackson<sup>1</sup> reporting a melting point ( $T_m$ ) of  $610^\circ\text{C}$ . Our results<sup>2</sup> using 1-chloronaphthalene solution polymerized PpPT, usually of lower molecular weight than the melt-polymerized material, agree; no transition is seen at temperatures up to  $450^\circ\text{C}$ . The asymmetric poly(*p*-oxybenzoate) (PpOBA), with all ester groups in the same direction, has a  $T_{k-m}$  of  $325\text{--}260^\circ\text{C}$ , depending on the morphology as determined by the method of polymerization<sup>3,4</sup>. Likewise, the copolymer poly(phenyl *p*-phenylene terephthalate) (PPpPT), prepared from phenylhydroquinone, in which the phenyl branches are randomly positioned on the alternating dioxyphenyl residues of the PpPT molecule, has a  $T_{k-m}$  of  $325\text{--}340^\circ\text{C}$ <sup>5,6</sup>, while the terpolymer of phenylhydroquinone, acetoxybenzoic acid and terephthalic acid has an even lower<sup>7</sup>  $T_{k-m}$ . Here, we consider two polymers similarly related to poly(4,4'-oxybiphenylencarbonyl) (POBC)<sup>8</sup> and poly(2,6-oxynaphthoyl) (PONY)<sup>9</sup>, namely poly(3-phenyl-4-oxybiphenylene-4'-carbonyl) (PPOBC) and poly(5-phenyl-2-oxy-6-naphthoyl) (PPONY). In contrast to PPpPT, the

phenyl rings on the polymers considered here are regularly positioned along the chain. As will be shown, this permits the development of a high degree of crystallinity and a high  $T_{k-m}$ , higher than that for the related polymer.

We describe here both the physical characterization of bulk melt-polymerized PPOBC and PPONY and the morphology and crystal structure of samples prepared by confined thin film melt polymerization (CTFMP). Details of the CTFMP process, as applied to PpOBA, are described elsewhere<sup>10</sup>. The CTFMP results extend our prior CTFMP studies of all of the above polymers. In most cases, lamellae ca.  $100 \text{ \AA}$  ( $1 \text{ \AA} = 0.1 \text{ nm}$ ) thick are produced.

## EXPERIMENTAL

The PPOBC and PPONY monomers (3-phenyl-4-acetoxy-4'-carboxybiphenyl ( $T_m = 274^\circ\text{C}$ ) and 5-phenyl-6-acetoxy-2-carboxynaphthoyl ( $T_m = 236^\circ\text{C}$ ), respectively) were prepared as described elsewhere<sup>11</sup>. For the CTFMP samples, the monomers were cast from acetone solution (ca. 1% concentration) onto a glass cover slip and covered with another glass plate when dry. They were then heated on a thermostatted hot plate at polymerization temperatures ( $T_p$ ) of  $200\text{--}250^\circ\text{C}$ , i.e. in most cases below the  $T_m$  of the monomers (see elsewhere<sup>10</sup>). For electron microscopy (EM) and electron diffraction (ED), samples were rinsed with acetone, then platinum or carbon shadowed and carbon coated, and then removed from the cover slips by floating on HF. The samples were then picked up on EM grids. Observation was done on a Philips EM400 or Hitachi 600 EM, with gold used for ED calibration. A Philips hot stage was used for high temperature studies.

\* To whom correspondence should be addressed

The unit cells were modelled using the Cerius<sup>2</sup> program (from Molecular Simulation Inc.) the Drieding force field; better agreement was obtained than with the Universal force field. A number of possible space group symmetries were tried for each of the polymers with minimization using the Minimizer module. Following minimization, the chain conformation developed was rebuilt in the crystal using the Crystal Builder module

and the selected space group symmetry; as suggested by the program, we performed slight rigid rotation and translation of the resulting molecular positions to improve the agreement with the observed patterns. The cells described give the best agreement with both the *hk0* single-crystal patterns and the less well defined ED fibre patterns from sheared samples.

Bulk-polymerized PPOBC and PPONY were prepared

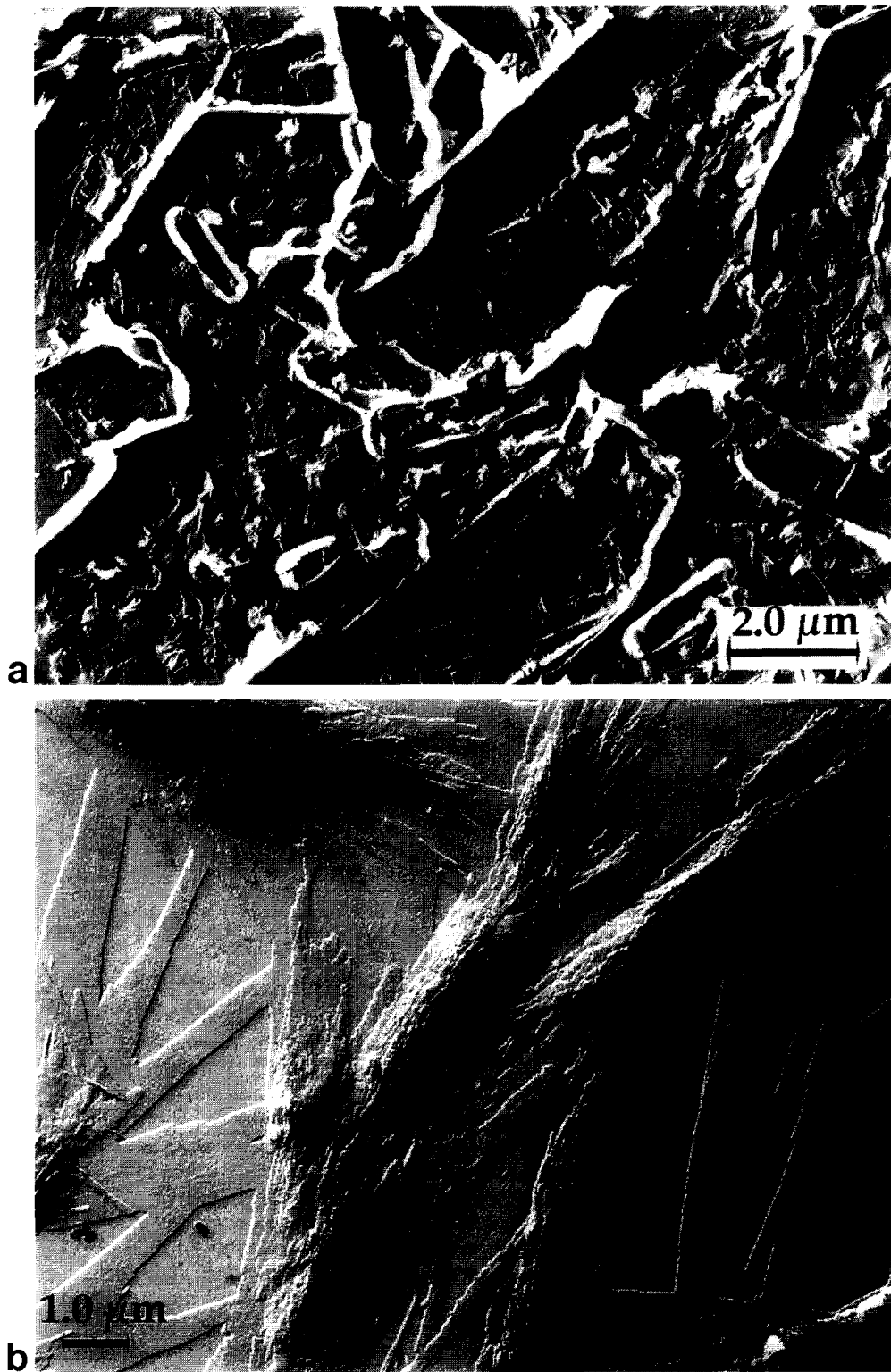


Figure 1 PPOBC polymerized at (a) 200°C for 18 h, (b) 240°C for 7 h and (c) 250°C for 4 h



Figure 1 (Continued)

from the monomers by stepwise heating. For PPOBC the conditions were 280°C for 1 h, 310°C for 30 min, 350°C for 2 h and 370°C for 5 h, all at 1 atm, followed by 380°C for 1 h at 1 mmHg. For PPONY, the conditions were 250°C for 1 h, 260°C for 30 min, 290°C for 50 min, 320°C for 40 min, 350°C for 1 h, 380°C for 1 h and 390°C for 5 h, followed by 390°C for 1 h at 1 mmHg.

These samples were examined by X-ray diffraction using a Rigaku Denki Geiger Flex D-Max IIIa with CuK $\alpha$  radiation at room temperature and at elevated temperature, in the latter case on a Mettler FP-5 hot stage.

## RESULTS AND DISCUSSION

### PPOBC

Figure 1 shows the lamellar morphology of PPOBC polymerized at 200°C, 240°C and 250°C. At a 200°C polymerization temperature, the lamellae appear less perfectly organized than at 240°C and 250°C. A basal lamella appears to cover the substrate, on which the other lamellae grow. The elongated ring-type structures were frequent. On occasion they were found with a top film at least partially complete, giving the suggestion they were 'bubbles'; this film was also lamellar. It is suggested that rinsing with acetone caused decomposition of this film on most of the bubbles. In this 200°C sample the acetone also etched some of the lamellae, again indicative of the low molecular weight. We have no explanation, however, for the elongated shape of the 'bubbles'. In all three micrographs the basal lamellae are ca. 50 Å thick, corresponding to a degree of polymerization ( $DP$ ) of 5, with thinner overlying lamellae being present on the samples in Figures 1b and 1c. In thicker portions of the film for both a 240°C and 250°C  $T_p$ , the lamellae are

organized into spherulitic structures (Figure 2). Again, the basal lamellae (ca. 100 Å thick) are well defined, while the overlying lamellae are less well defined.

The thinness of the lamellae raises the question as to whether the sample should be considered polymeric. An X-ray scan of bulk-polymerized PPOBC is shown in Figure 3, with ED patterns of the CTFMP sample in Figure 4. The spacings agree. As shown in Figures 4a and 4b (two different camera lengths), there are weak reflections half way between the primary reflections on both the  $h00$  and  $h10$  row lines, suggesting a possible doubling of the unit cell in the  $a$  axis direction. In addition to  $kh0$  single-crystal patterns,  $h0l$  single-crystal patterns were also obtained from the as-polymerized samples (Figure 4c). The  $h = n + 1/2$  reflections are not visible on these patterns. The morphological origin of the  $h0l$  patterns has not been determined; possibly they are related to the lamellae on their edges in Figure 1a. The lamellae on the edges of the spherulitic structures give rise to  $hk0$  patterns, as in Figures 4a and 4b. A monoclinic (pseudo-orthorhombic) unit cell with  $a = 15.24$  Å (or 30.48 Å),  $b = 3.94$  Å and  $c = 10.54$  Å is indicated; the space group is  $Pn$  with unique axis  $a$ , and  $\alpha = 90^\circ$ . As indicated by Figure 4a, there is a high degree of perfection to the cell, spacings being observable out to 1300 (i.e. 0.8 Å) in the  $a$  axis direction and the  $h30$  row line in the  $b$  axis direction. The value of  $c$  is essentially the same as for phase I POBC (10.8 Å);  $c$  is not known for phase II POBC<sup>8</sup>. In Figure 4c there is a suggestion that 005 is doubled along the meridian (see Figure 8 later). This could arise from a different unit cell but none of the other reflections appears to be doubled in the  $c$  axis direction, although their azimuthal width would make this difficult to observe for any but the 001 reflections.



Figure 2 'Spherulitic' clustering of lamellae on their edges in PPOBC prepared by CTFMP (250°C, 4h)

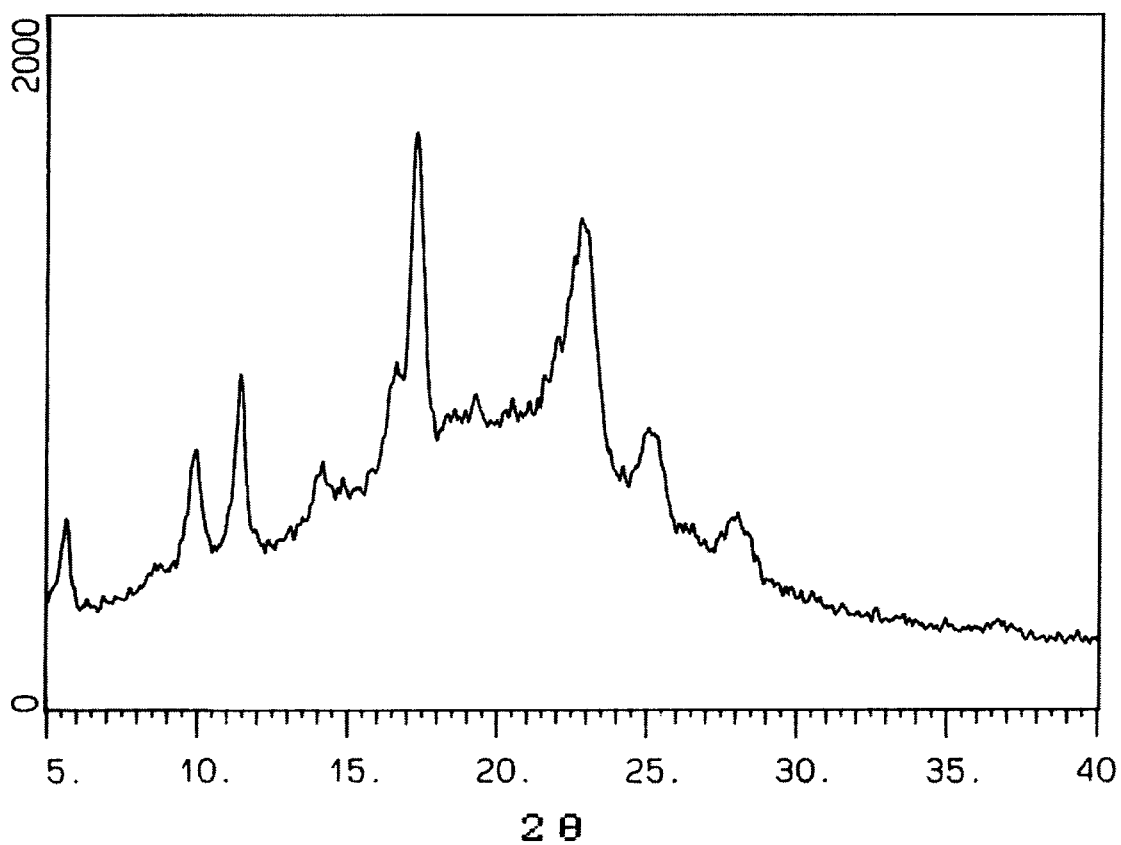
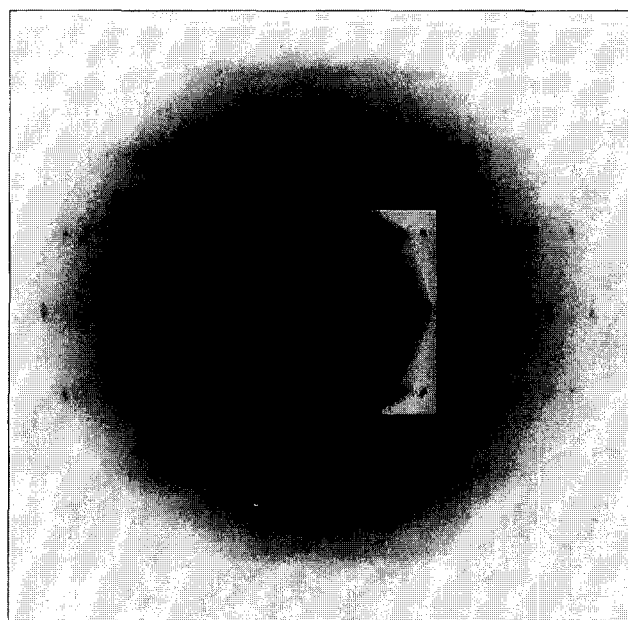
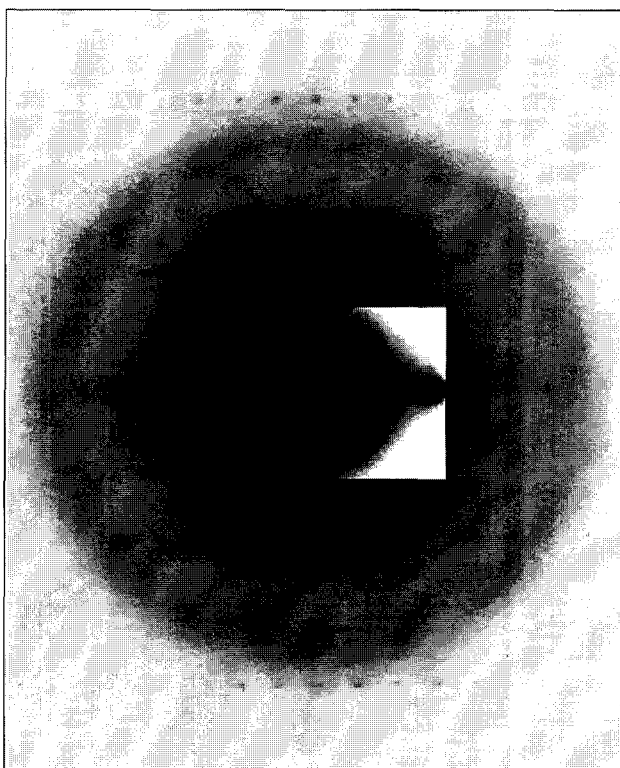


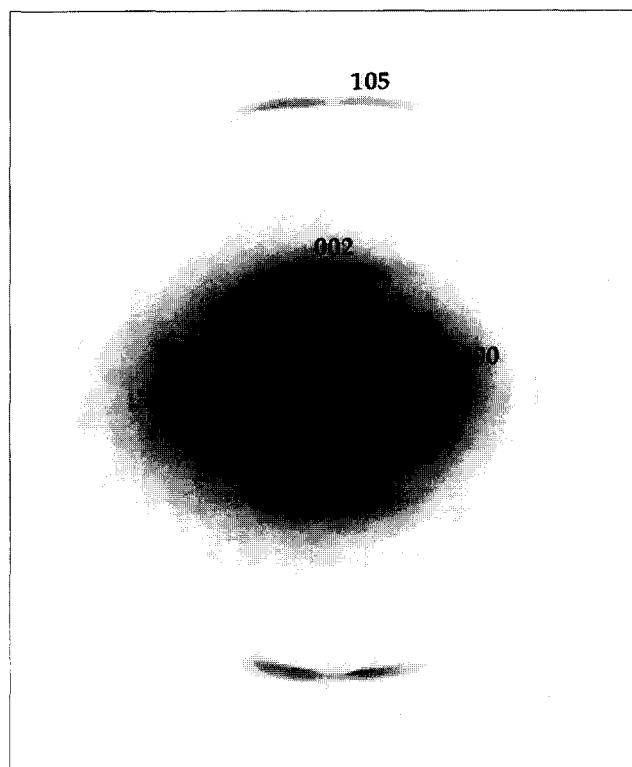
Figure 3 An X-ray diffraction scan from a sample of bulk-polymerized PPOBC



a



b



c

**Figure 4** ED patterns from PPOBC prepared by CTFMP at 250°C over 4 h. Both  $hk0$  (a, b) and  $h0l$  (c) patterns are obtained. Parts (a) and (b) are from two different areas, with different exposure times and camera lengths (the strong  $\{110\}$  and  $\{210\}$  reflections in (b) are just visible on the left-hand side of the central inset in (a)). In (c), only  $h00$  reflections are seen on the equator

The molecular packing suggested by the Cerius<sup>2</sup> program is shown in *Figures 5a–c*. As for POBC,  $c$  corresponds to a single chemical repeat unit. The backbone phenyl rings are only slightly twisted with respect to each other, while the side-chain phenyl rings interleave and are tilted at an angle to the  $c$  axis. The corresponding density is  $1.429 \text{ g cm}^{-3}$ . The corresponding  $[001]$  diffraction pattern is shown in *Figure 5d*; it agrees well with the intensity distribution observed (*Figures 4a* and *4b*) other than for the  $h = n + 1/2$  reflections. The presence of 1200 in *Figure 4a* is attributed to double diffraction with 600 being the incident beam. The  $[010]$  zone (*Figure 5e*) also agrees well with the pattern shown in *Figure 4c*, assuming that the fifth layer line reflections are 105 and not 005, the azimuthal width of the reflections causing their emergence. On the negative there is a minimum of intensity on the meridian. *Figure 5f* shows the expected ED pattern from a fibre. ED patterns are not shown for the sheared samples of this polymer; as shown below for PPONY, they usually contain many fewer (and broader) reflections than the patterns from the as-polymerized material. The patterns from the sheared samples were similar to the pattern in *Figure 8b*, the  $h0l$  patterns taking on a 'fibre' character when the sample is heated.

A differential scanning calorimetry (d.s.c.) scan of the bulk-polymerized material is shown in *Figure 6*. A single transition at 422°C is seen. The X-ray pattern (*Figure 3*) suggests a relatively low degree of crystallinity. In the bulk-polymerized samples the transition heat suggests it is a crystal–nematic transition. The peak near 490°C is attributed to degradation. Other than for an apparent gradual decrease in the number of observable reflections (possibly owing to faster beam damage) and an increase in lattice parameters, there was no change in the  $hk0$  ED patterns up to 370°C (*Figure 7*). Although it appears in

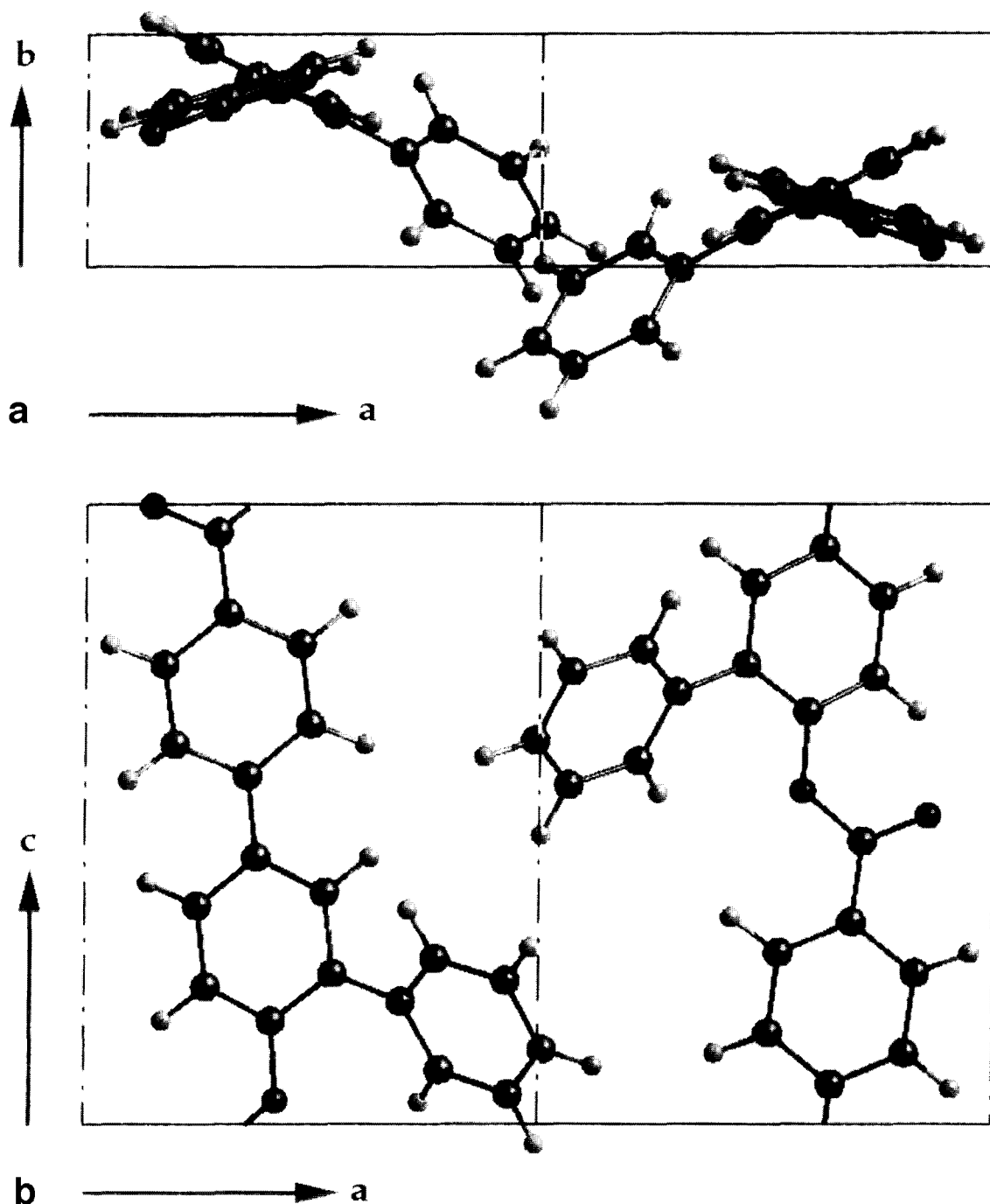


**Figure 5** (a–c) Unit cell packing for PPOBC as minimized by the Cerius<sup>2</sup> program for the  $Pn11$  space group. (d) The [001] ED pattern corresponding to (a). (e) The [010] ED pattern corresponding to (b). (f) The simulated ED fibre pattern

Figure 7a that the outer reflections are becoming smeared, and in Figure 7b only a few reflections are visible, sharp spots were still present out to 420 on the  $h20$  row line at 266°C. At least one of the  $h = n + 1/2$  reflections visible in Figures 4a and 4b was still visible up to 290°C, although they were not visible in the negative for Figure 7a.

Above 370°C the reflections disappear, only an amorphous (nematic) ring being obtained. Cooling the sample to room temperature, however, after heating to 390°C results in a regeneration of the crystal lattice (Figure 7c) with the same spacings as in the nascent

polymer. The lower  $T_{k-m}$  than for the bulk-polymerized sample is attributed to the lower molecular weight.

On heating the crystals, we found that the original  $h0l$  ED patterns took on a fibre character, i.e. 110 as well as  $h00$  reflections were present on the equator (Figure 8a). Quadrant reflections were retained. The doubling of 105, just visible in Figure 4c, is clearly visible in Figure 8a; 002 does not appear to be doubled. Although we have seen similar doubling in ED fibre patterns from other liquid crystal polymers, we have no confirmed explanation at present. Here, it may be due to diffraction from both the

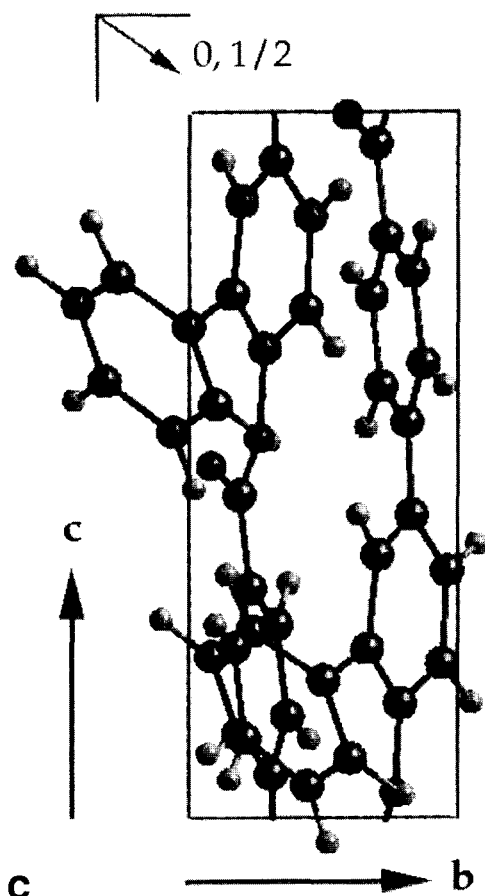


Figure 5 (Continued)

crystal and oriented liquid crystal regions. Although reflections out to  $0010$  are visible on the negative, they are too weak to determine if they are doubled. Broad, diffuse scatter centred on the equator and in the quadrants at ca.  $0.84 \text{ \AA}^{-1}$  ( $1.19 \text{ \AA}$ ), forming a hexagonal pattern, can also be attributed to the oriented nematic material; the spacing corresponds closely to the '100' spacing ( $1.21 \text{ \AA}$ ) in the aromatic rings. While such a spacing can be observed from the carbon substrate, it is a diffuse ring.

Cooling the sample to room temperature after heating to  $390^\circ\text{C}$  in the electron microscope results in considerable diffuseness in the pattern (Figure 8b). Although  $h00$  and some quadrant reflections remain sharp, 'amorphous' equatorial scatter occurs between 200 and 300 and the  $00l$  reflections also become diffuse; doubling of 105 was not apparent. We attribute this diffuse scatter to the presence of a considerable degree of oriented amorphous or glassy nematic material.

Heating the sample to above  $T_{k-m}$  followed by quenching results in a complete loss of the lamellar texture. Figure 9 is a micrograph of such a sample, originally a thicker film as in Figure 2, that was quenched from ca.  $425^\circ\text{C}$ . This sample was heated, on the grid, on the hot stage of the electron microscope before shadowing. Not only is the lamellar texture gone, but fibres are drawn across the cracks in the regions originally consisting, it is believed, of lath lamellae. The cracks are attributed to the mesophase-crystal transformation, the fibres and loss of lamellar texture to rapid end linking above  $T_{k-m}$  (due to the 'proper' orientation

of the chain ends) and the resultant high molecular weight.

#### PPONY

Lath-like lamellae are also formed during the CTFMP of PPONY. Figures 10a and 10b show the results of polymerization at  $250^\circ\text{C}$  for 4 h and 18 h, respectively. The basal lamellae are of the order of  $100 \text{ \AA}$  in thickness for both samples, with the overgrowths in Figure 10b being somewhat thinner. As shown by the inset ED pattern in Figure 10b, from the lath in the centre of the micrograph, the  $b$  axis is parallel to the long axis of the lath; this also is the result for PPOBC.

The basal lamellae are the same thickness and merge when they meet (e.g. Figure 10a), suggesting they are growing on the substrate; overlying lamellae from one of the basal lamellae may then grow over the opposite members of the merged pair without loss of orientation, i.e. the orientation of overlying lamellae is not determined by the underlying lattice. In both micrographs the end of the laths are split into narrower, sometimes slightly tapered sections. Frequently seen are narrow lath sections, of near uniform width, lying on the crystals. All of this suggests growth is in the  $b$  axis direction predominantly.

In thicker portions of the film, as in Figures 10b and 11a ( $T_p = 200^\circ\text{C}$ , 18 h), the lath crystals twist up from the substrate. Although it was not possible to obtain ED patterns from the material, it is believed the molecules are parallel to the substrate. The flat-on lath crystals in this sample again have tapered ends and overlying narrow lath sections. In other portions of this  $200^\circ\text{C}$   $T_p$  sample, aggregates of what appear to be lamellae on their edges are seen (Figure 11b); they do not appear to develop from twisting of the lath lamellae. In both Figures 11a and 11b, the lamellar nature of the thick laths is difficult to see owing to the overlying narrow lath sections; it can be seen most easily at the ends of the laths (arrows). Polymerization at  $210^\circ\text{C}$  and  $220^\circ\text{C}$  yielded similar structures. At  $180^\circ\text{C}$ , however, the irregular edge-on lamellae were often organized in parallel arrays (Figure 12). An apparent 'substrate' of lath lamellae, however, was still present.

An ED pattern from the lath crystals is shown in Figure 13a. It indicates an orthorhombic (see Figure 13b) unit cell with  $a = 29.60 \text{ \AA}$  and  $b = 5.08 \text{ \AA}$ , i.e.  $a$  again is very large. As we have observed for a number of other liquid crystal polymers both grown by CTFMP (see Figure 12d in the paper by Rybnikar *et al.*<sup>10</sup>) and by crystallization from the nematic state<sup>12</sup>, a single  $\{hk0\}$  reflection, here  $\{510\}$ , is radially split; we still have no explanation for this phenomenon. This type of splitting was not observed for PPOBC.

In order to obtain  $c$  we scraped the PPONY samples from the cover slips and sheared them at ca.  $320^\circ\text{C}$  with a razor blade. Although fibre patterns were obtained, their sharpness was improved by annealing (Figure 13b). These patterns are as good as or better than those we have obtained by shearing and annealing PONY<sup>13</sup>, again indicating the high degree of crystallizability of these polymers. In contrast to PONY, for which 002 and 008 are strong while 004 and 006 are weak, 004 here is stronger than 008. The value of  $c$ ,  $16.74 \text{ \AA}$ , is smaller than found for PONY ( $17.0$ – $17.5 \text{ \AA}$  from Schwarz and Kricheldorf<sup>14</sup>,  $17.1 \text{ \AA}$  from Iannetti *et al.*<sup>15</sup> and  $17.4 \text{ \AA}$  ( $d_{002} = 8.68 \text{ \AA}$ , monoclinic cell) from Liu *et al.*<sup>9</sup>).

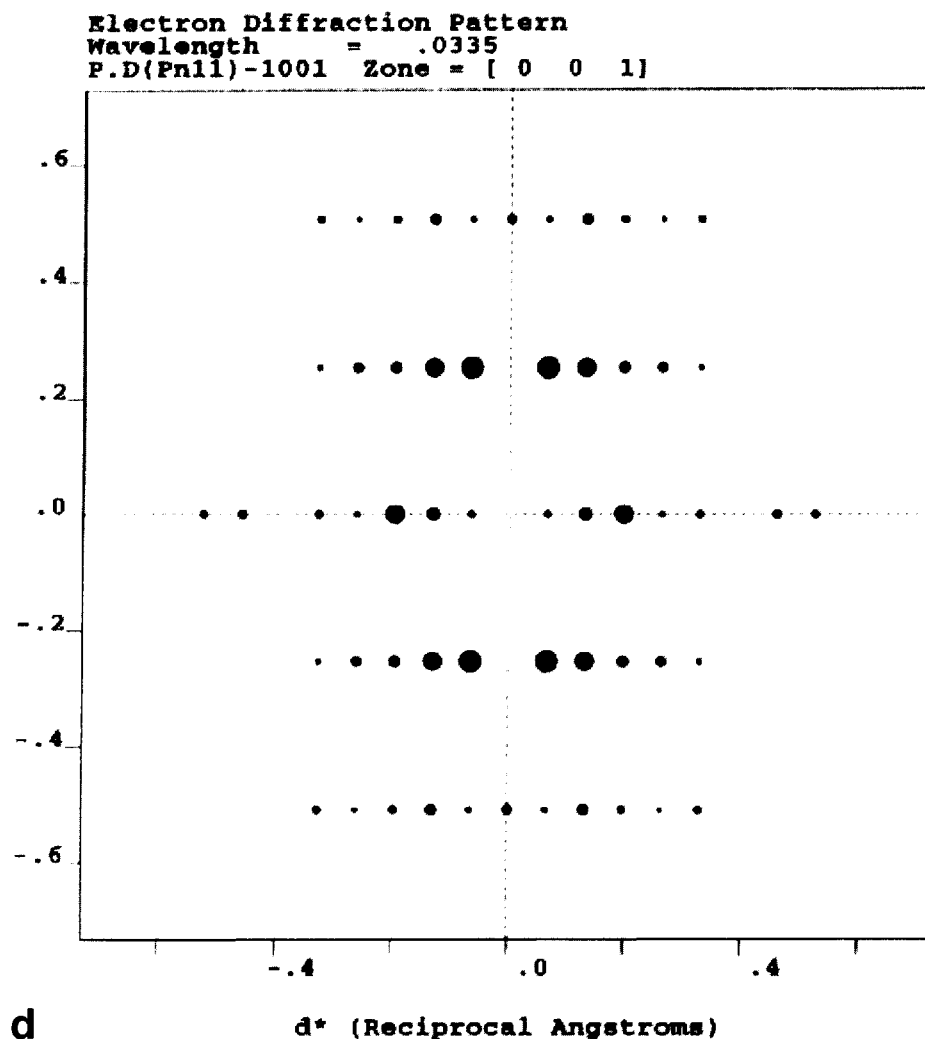


Figure 5 (Continued)

The orthorhombic unit cell suggested by the Cerius<sup>2</sup> modelling is shown in Figures 14a–c. The space group is  $P2_1/c2_1/c2/n$ . Pairs of molecules act as single units with the phenyl rings again interleaved. Comparison of the corresponding simulated [001] ED pattern (Figure 14d) with the pattern obtained experimentally (Figure 13a) shows good agreement except for the near absence of 020 and 220 (0.01% and 0.42% of  $I_{400}$ , respectively); we attribute the higher observed intensity to a slight degree of double diffraction, {110} and {310} serving as incident beams. A simulated fibre pattern is shown in Figure 14e; the agreement with Figure 13b is good within the limitations of the few reflections in Figure 13b. In particular, the agreement with the relative intensities of the 00l reflections is good. The calculated density is  $1.300 \text{ g cm}^{-3}$ .

An X-ray scan of the bulk-polymerized material is shown in Figure 15. The spacings agree with those from the ED patterns, again indicating that the chain length of the CTFMP material is sufficient to give a polymer-type unit cell. The crystallinity of the bulk PPONY is considerably higher than that of PPOBC.

A d.s.c. scan of the bulk material is shown in Figure 16. A small endothermic peak is seen at 334°C, with a larger peak at 529°C, degradation occurring above 550°C. The origin of the 334°C peak is not yet known. As shown in Figure 17, the intensity of X-ray scans taken on a hot stage increases significantly when the sample is heated to

300°C, but the only change when the sample is heated above 335°C is in the peak at 17°; it appears doubled at 300°C and is both weaker and single at 360°C. The spacing of this peak (4.93 Å at room temperature) corresponds to the 600 and 110 reflections in the ED pattern, both of which are strong.

ED patterns taken at elevated temperature also show no change in the vicinity of 335°C (Figure 18). However, between ca. 130°C and 260°C, diffuse pairs of reflections (similar to our observations for PpPT<sup>6</sup>) are seen on the  $h(k + 1/2)0$  row lines (Figures 18a and 18b). These reflections do not lie on vertical row lines, but rather half way along lines connecting reflections on the horizontal row lines. By 500°C the regular reflections have become somewhat more diffuse (Figures 18c and 18d), with fewer orders visible and lattice expansion ( $a = 30.8 \text{ Å}$ ,  $b = 5.6 \text{ Å}$ ). They disappear, with a diffuse (nematic or amorphous) halo being present at ca. 550°C, in agreement with the d.s.c. results. It is noted that the temperatures listed for the hot stage ED patterns are only approximate. We have no way to calibrate the temperature *in situ*.

The heating cycle to 550°C, as for PPOBC, results in the loss of the lamellar texture and the development of cracks bridged, in some cases (arrows), by fibres (Figure 19). Both the lath lamellae and the aggregates become more homogeneous, attributed again to end linking of the original oligomers.



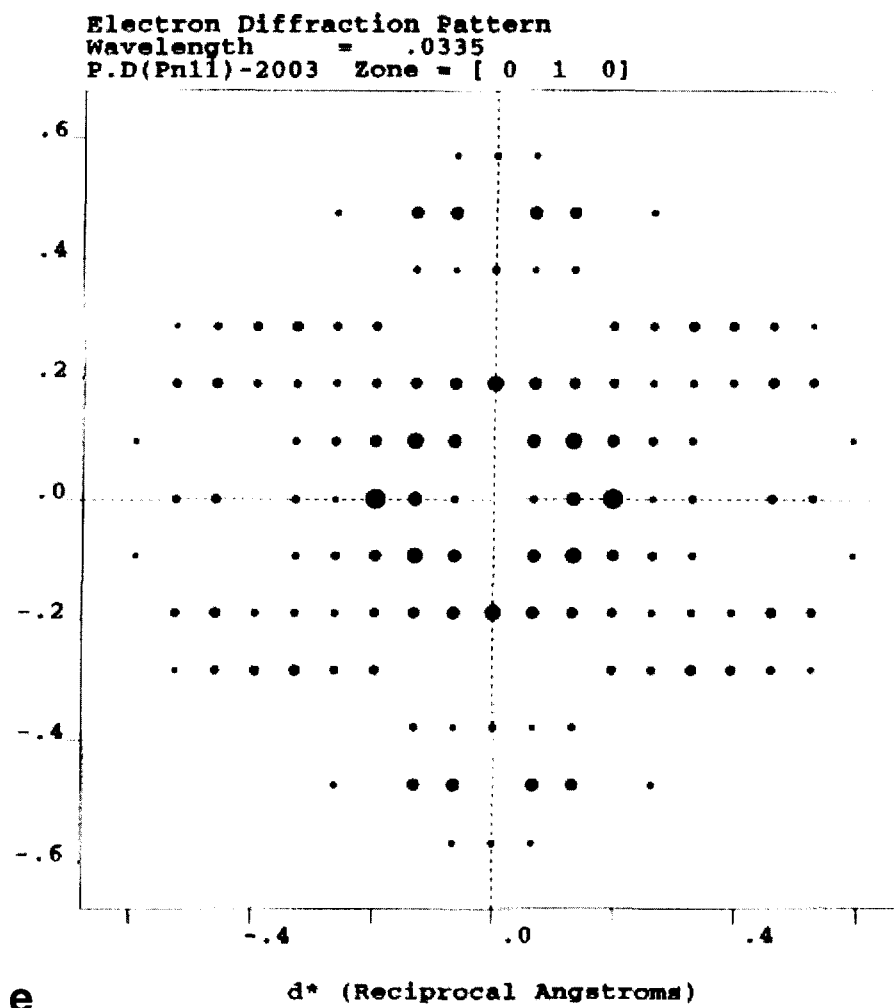


Figure 5 (Continued)

## CONCLUSIONS

1. PPOBC and PPONY both form highly perfect lamellar oligomer crystals by the CTFMP process. These crystals have permitted determination of the unit cell parameters:

- (a)  $Pn11$ ,  $a = 15.24 \text{ \AA}$ ,  $b = 3.94 \text{ \AA}$ ,  $c = 10.54 \text{ \AA}$  and  $\alpha = 90^\circ$  for PPOBC; and  
(b)  $P2_1/c2_1/c2_1/n$ ,  $a = 29.60 \text{ \AA}$ ,  $b = 5.08 \text{ \AA}$  and  $c = 16.74 \text{ \AA}$  for PPONY.

The  $c$  axis length for PPOBC is close to the value for the corresponding non-phenyl branch containing polymer POBC ( $10.8 \text{ \AA}$ )<sup>8</sup>, whereas that for PPONY is significantly shorter (see above; 002 has an  $8.68 \text{ \AA}$  spacing,  $c$  being  $17.4 \text{ \AA}$  in our monoclinic unit cell<sup>9</sup>). However, both of the values stated correspond to phase I for the respective polymers, with the  $hk0$  patterns here more closely resembling phase II;  $c$  is not known for phase II for either POBC or PONY. POBC phase II has<sup>8</sup>  $a = 15.6 \text{ \AA}$  and  $b = 3.6 \text{ \AA}$ , while PONY phase II has<sup>9</sup>  $a = 11.6 \text{ \AA}$  and  $b = 3.8 \text{ \AA}$ , both assuming an orthorhombic cell. Thus, in PPOBC and PPONY  $b$  has slightly larger values than those in the non-phenyl-branched polymers, while  $a$  is slightly smaller for PPOBC and nearly three times as big for PPONY. This suggests a considerable difference in

packing from even phase II of the non-phenyl-branched polymers, since the modelling places the side chains in the  $a$  axis direction.

2. Annealing of the oligomer crystals at elevated temperatures results in chain extension by end linking. The rapidity of the reaction is suggested to be due to both the temperatures involved and the juxtaposition of the appropriate chain ends. Contrary to the case of  $P_p\text{OBA}$ <sup>10</sup>, for which we suggest the polymerization occurs with the carboxy end attached to the glass, with parallel packing of adjacent molecules in a given lamella for both unit cells, here we are suggesting antiparallel packing of the chains. End linking across lamellar interfaces may thus be more difficult, but still appears to occur readily. As in the case of  $P_p\text{OBA}$  and our other CTFMP samples, we have as yet no explanation for the well-defined lamellar thickness in a given polymer, a thickness that appears to be independent of both  $T_p$  and polymerization time.
3. D.s.c. indicates high  $T_{k-m}$  values for the two polymers,  $422^\circ\text{C}$  and  $528^\circ\text{C}$ , consistent with the perfection of the crystal lattice. However, it is noted that PPOBC when bulk polymerized had a low degree of crystallinity. In addition, there appears to be a small transition at ca.  $335^\circ\text{C}$  in PPONY. At this temperature the 600/110 double peak in X-ray scans decreases in intensity and becomes a single peak;

Fiber Diffraction  
Radiation used = ELECTRON  
Wavelength = .0335  
Tilt angle = .0000  
P.D(Pn11)-2005 FLAT-PLATE

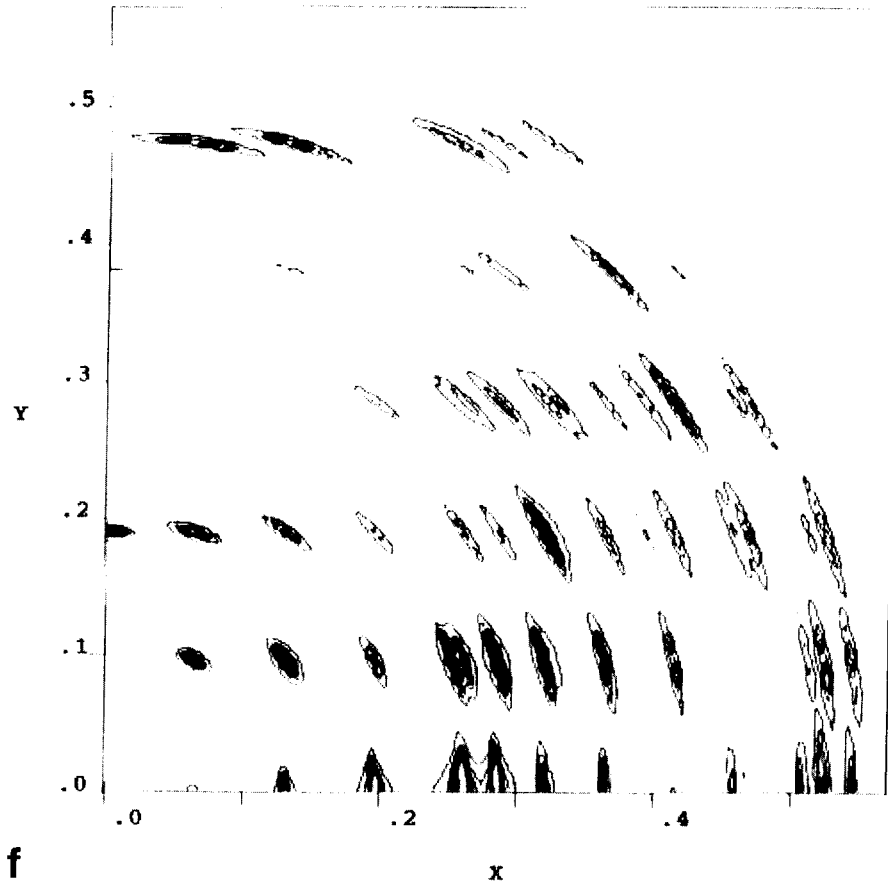


Figure 5 (Continued)

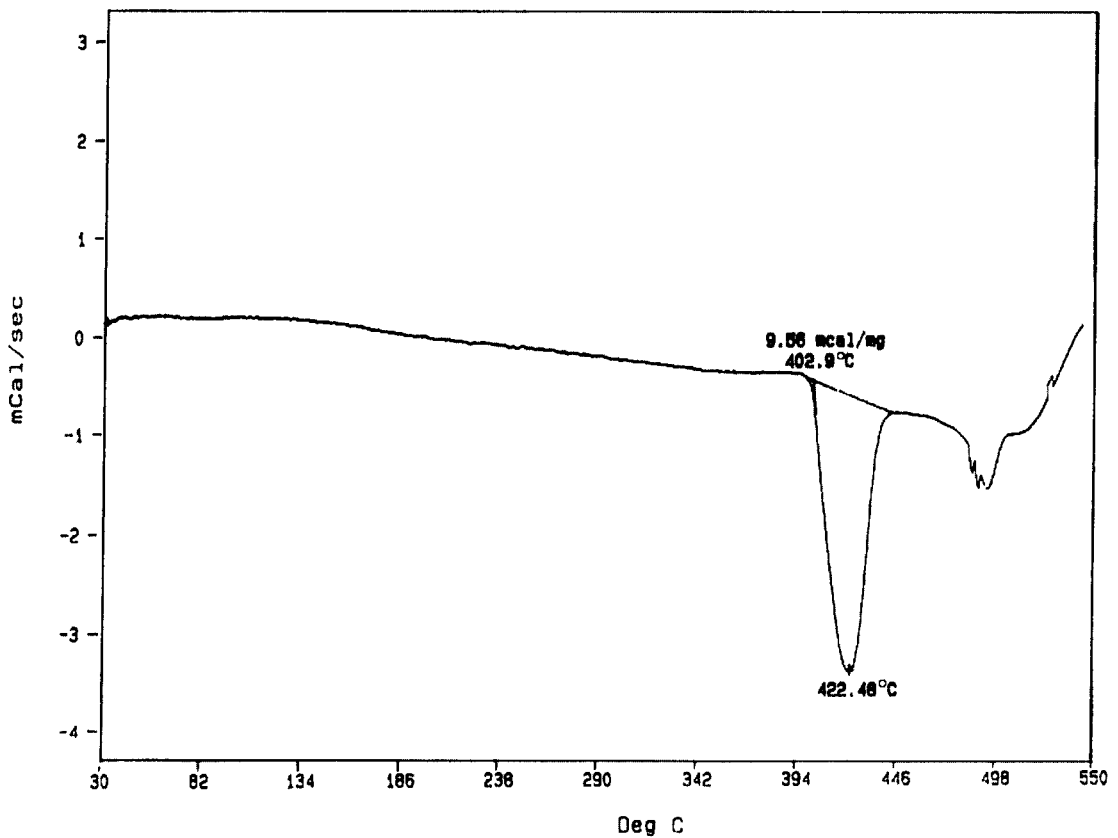


Figure 6 D.s.c. scan (second heating) of bulk-polymerized PPOBC

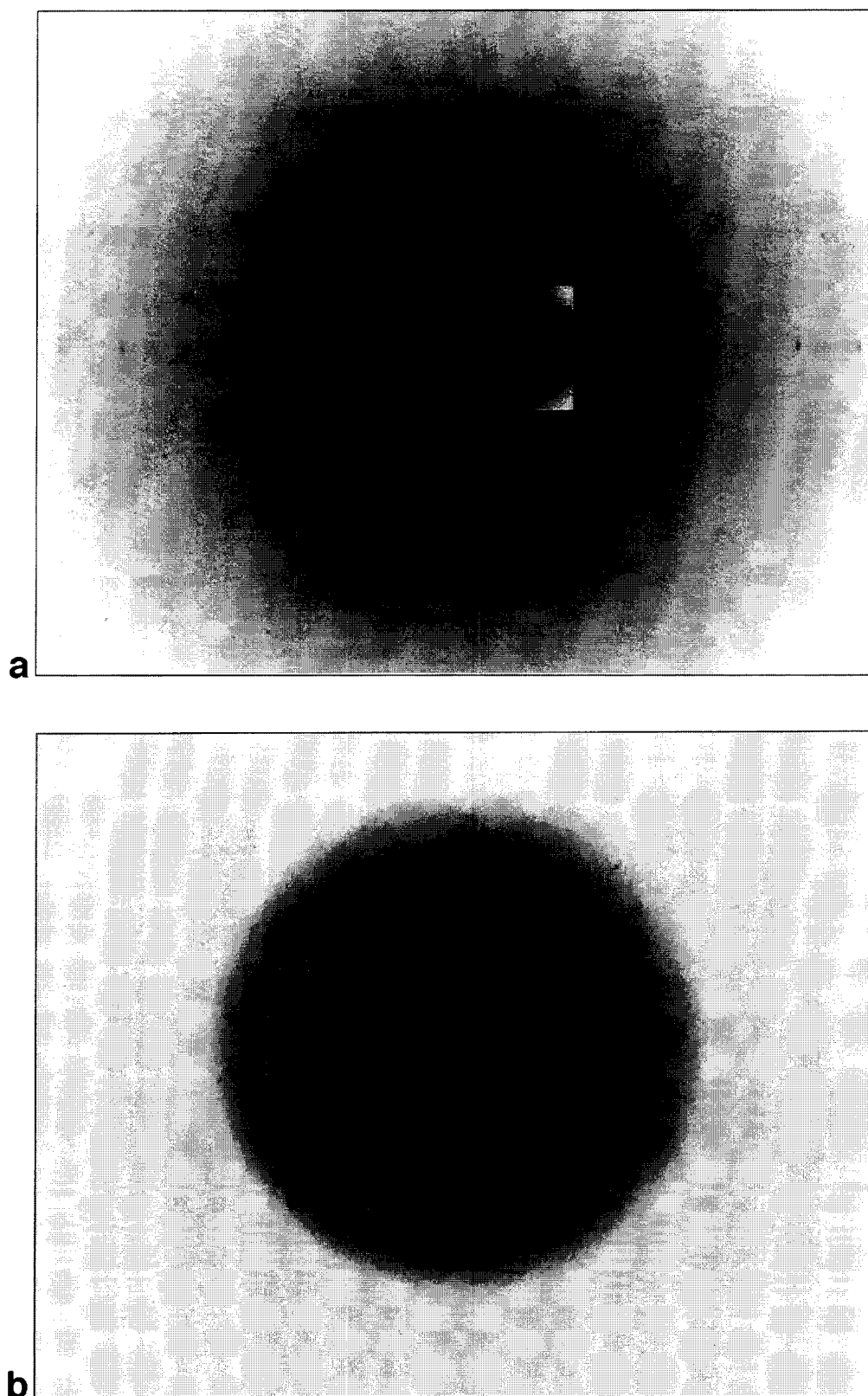


Figure 7 ED  $hk0$  patterns of CTFMP-prepared PPOBC (250°C, 4h) (a) at 250°C, (b) at 353°C and (c) after cooling from 390°C

however, no change is seen in the ED patterns. By ED (for which the temperatures are only approximate), the crystallinity is retained up to the above-stated  $T_{k-m}$ , after which only an amorphous (nematic) ring is seen. Cooling PPOBC from above this temperature

results in regeneration of the  $hk0$  single-crystal patterns, with a lower degree of crystal perfection and size than in the nascent polymer.

4. There are several, as yet unexplained, unusual features to the ED patterns.

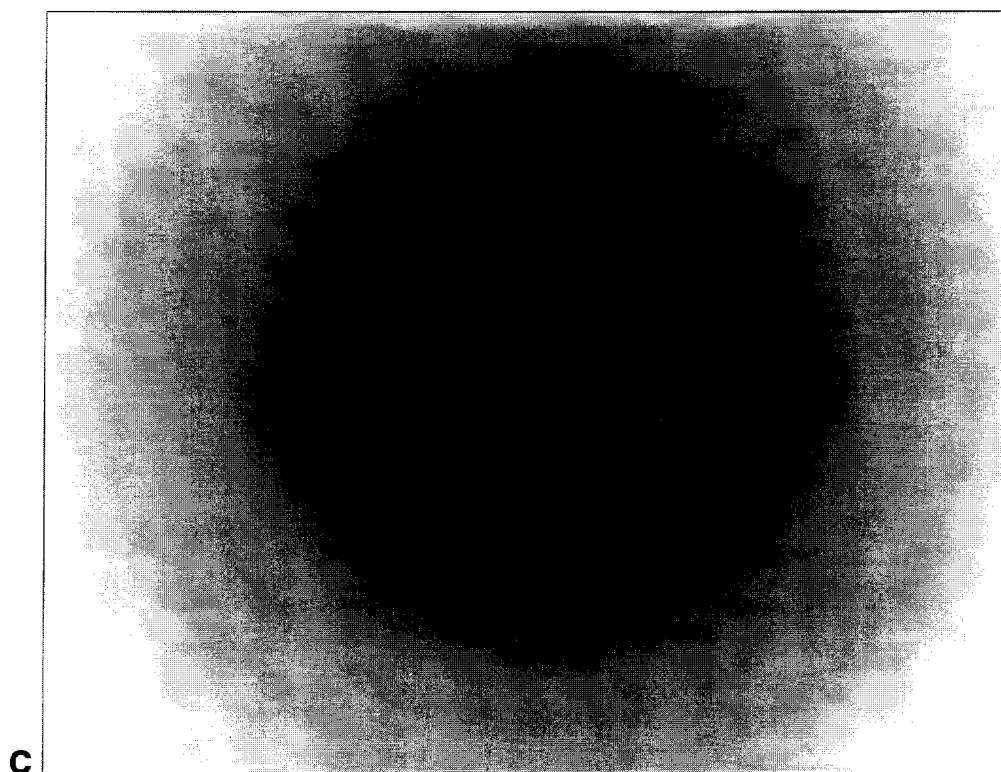


Figure 7 (Continued)

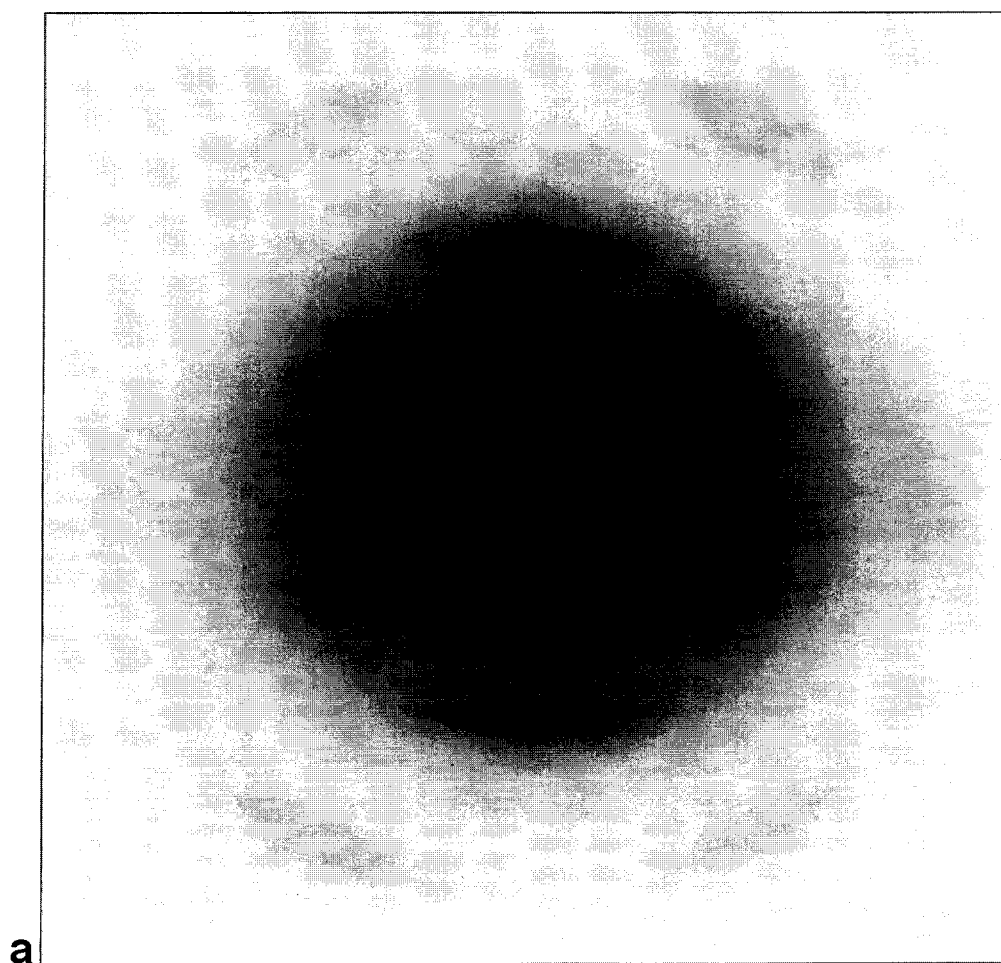
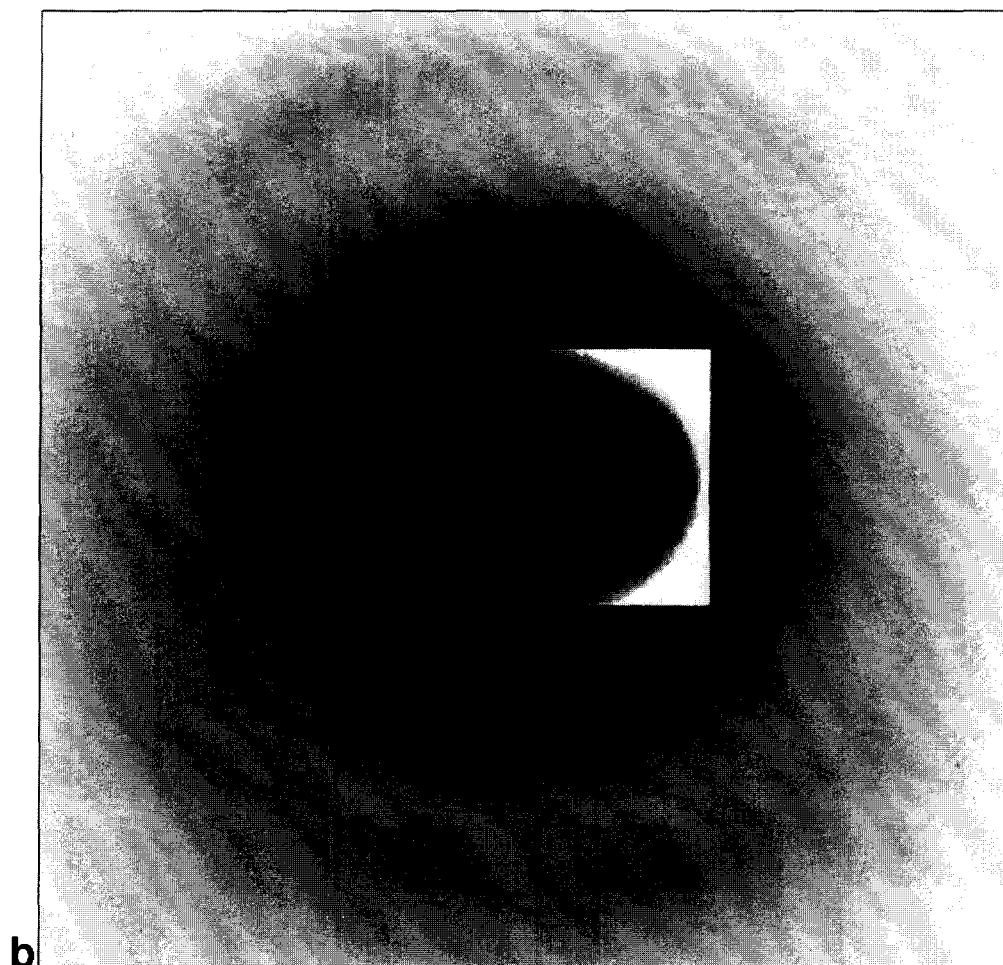
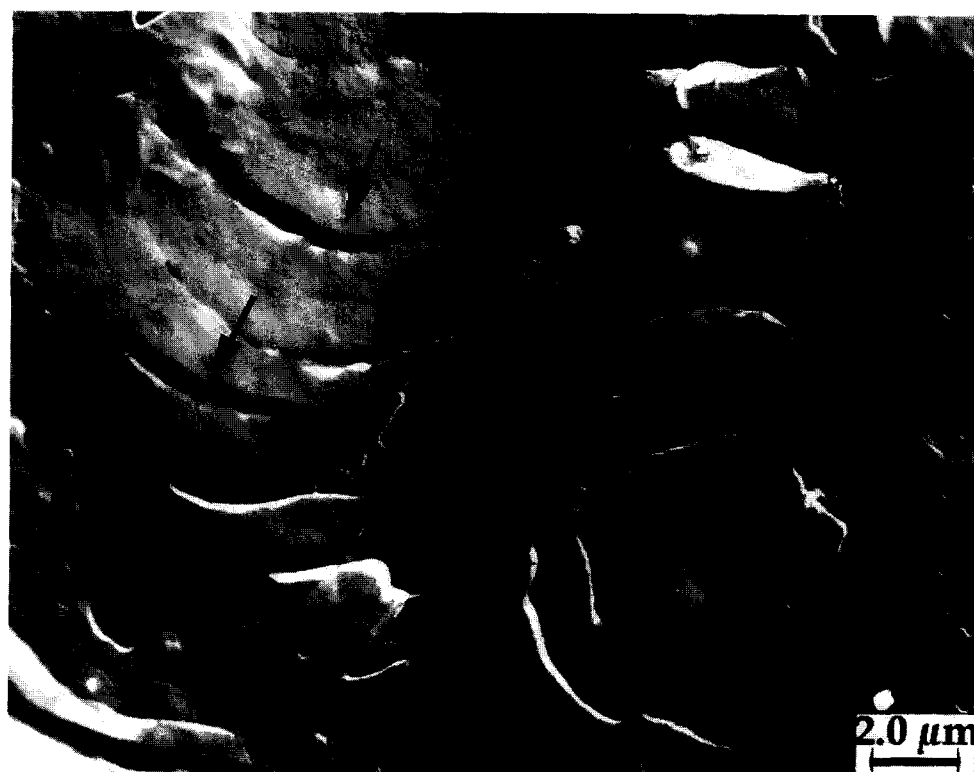


Figure 8 ED 'fibre' patterns of CTFMP-prepared PPOBC (250°C, 4h) (a) at 217°C and (b) after cooling from 390°C. In (a), the third strong equatorial reflection is 110



**Figure 8** (Continued)



**Figure 9** CTFMP-prepared PPOBC shadowed after cooling to room temperature from 425°C in the electron microscope hot stage. Fibres (arrows) can be seen drawn across many of the large and small cracks

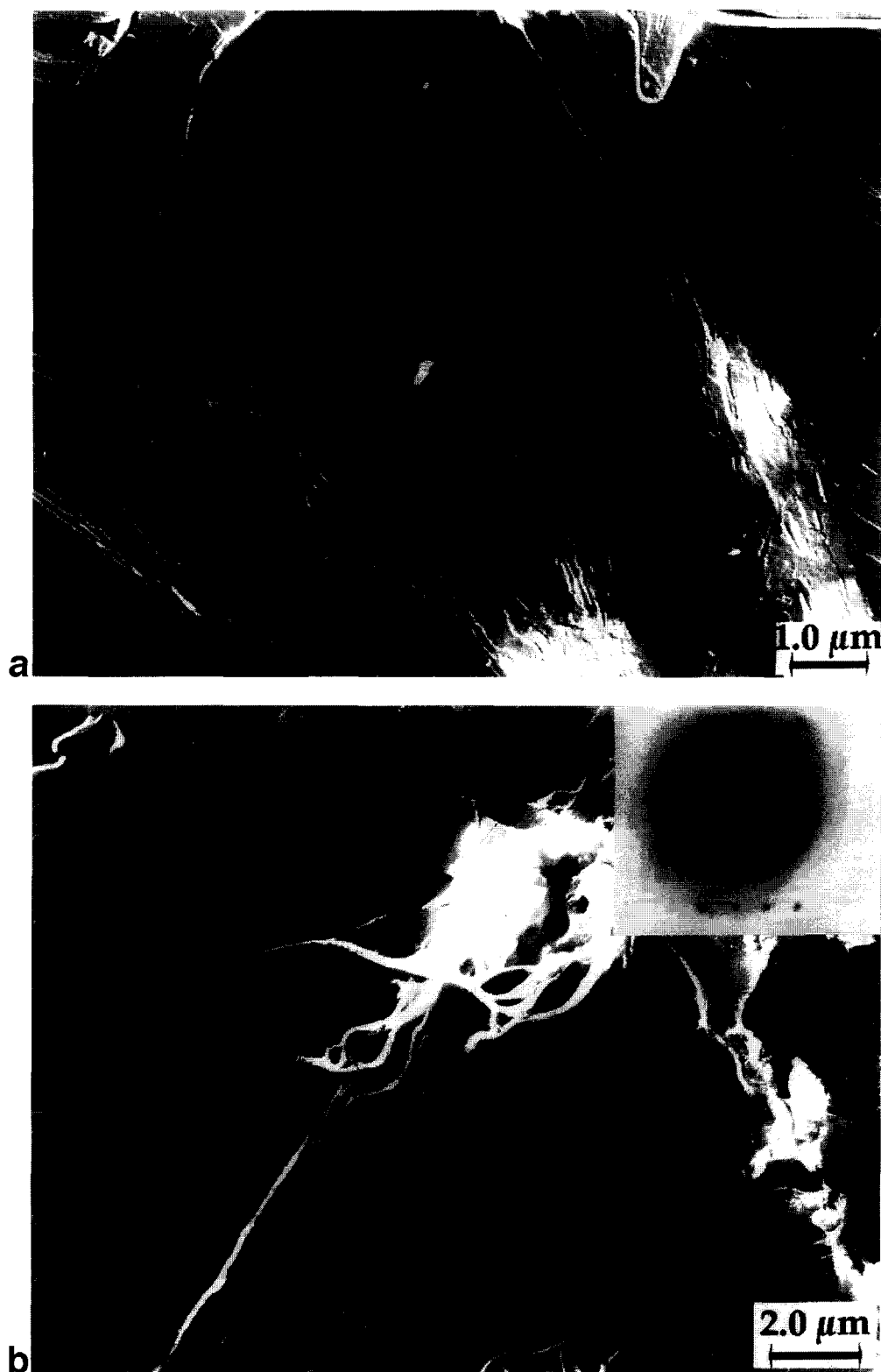


**Figure 10** Electron micrographs of CTFMP-prepared PPONY made at 250°C over (a) 4 h and (b) 18 h. The *b* axis of the inset ED pattern lies parallel to the long axis of the lath

- (a) There are weak reflections suggesting a doubling of the *a* axis for PPOBC. This doubling may be due to a pairing of molecules similar to that in PPONY.
- (b) There is a doubling of 105 in the *h0l* and 'fibre'

- patterns for PPOBC. This is possibly due to the superposition of crystalline and oriented nematic scattering.
- (c) There are pairs of extra reflections on the  $k = n + 1/2$  row lines in the *hk0* PPONY ED

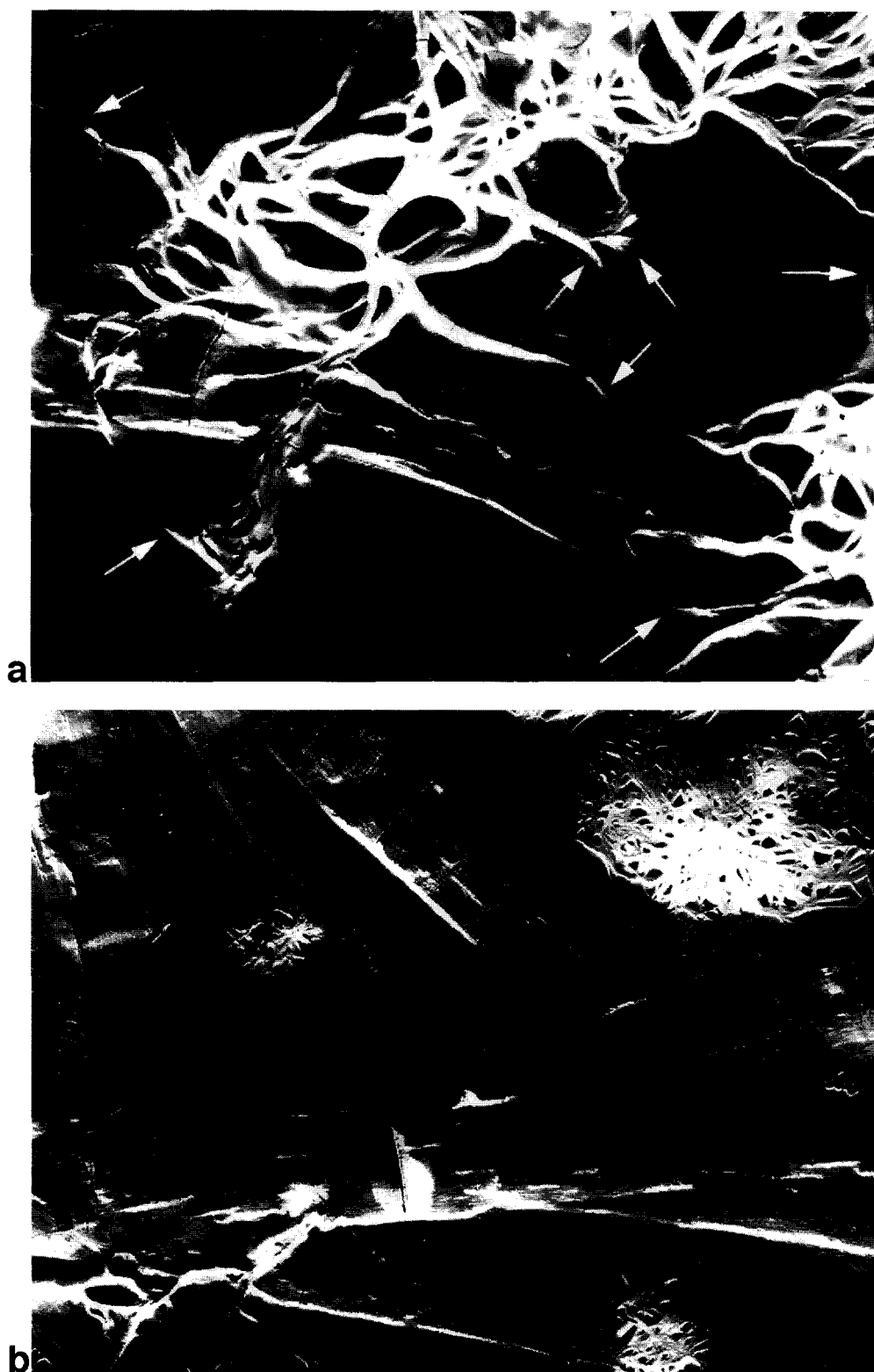


**Figure 11** CTFMP-prepared PPONY (200°C, 18h) showing lamellae twisting up from the substrate (a) and on their edges in aggregates (b). The arrows in (a) indicate lamellar edges visible at the ends of the laths

patterns, seen between at least 130°C and 260°C. Similar reflections were observed for one of the phases of PppPT at room temperature<sup>6</sup>. It is noted that their *a* axis spacings lie half way between those of the reflections on the neighbouring  $k = n$  and

$k = n + 1$  row lines. If these reflections are due to the intersection of the sphere of reflection with the 001 reciprocal lattice planes, due to molecular tilt, then they suggest a doubling of the unit cell in the *a* and *b* axis directions; this doubling is not seen in the

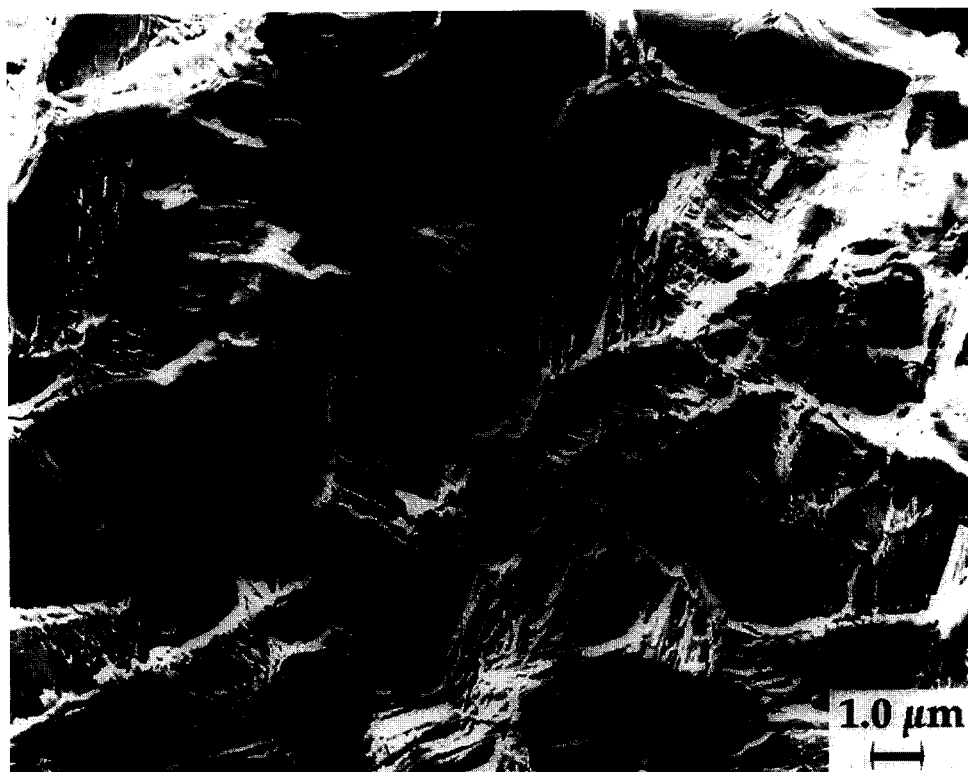


Figure 12 Parallel arrays of lamellae on their edges in CTFMP-prepared PPONY (180°C)

fibre patterns, with the entire first layer line having weak reflections. Rather, we suggest that some form of disordered superlattice may be present.

(d) There is a radial doubling of the single  $\{510\}$

reflections for PPONY. A similar effect, usually for  $\{210\}$ , has been seen for a number of other liquid crystal polymer single crystals<sup>5,12</sup>, with no explanation as yet.

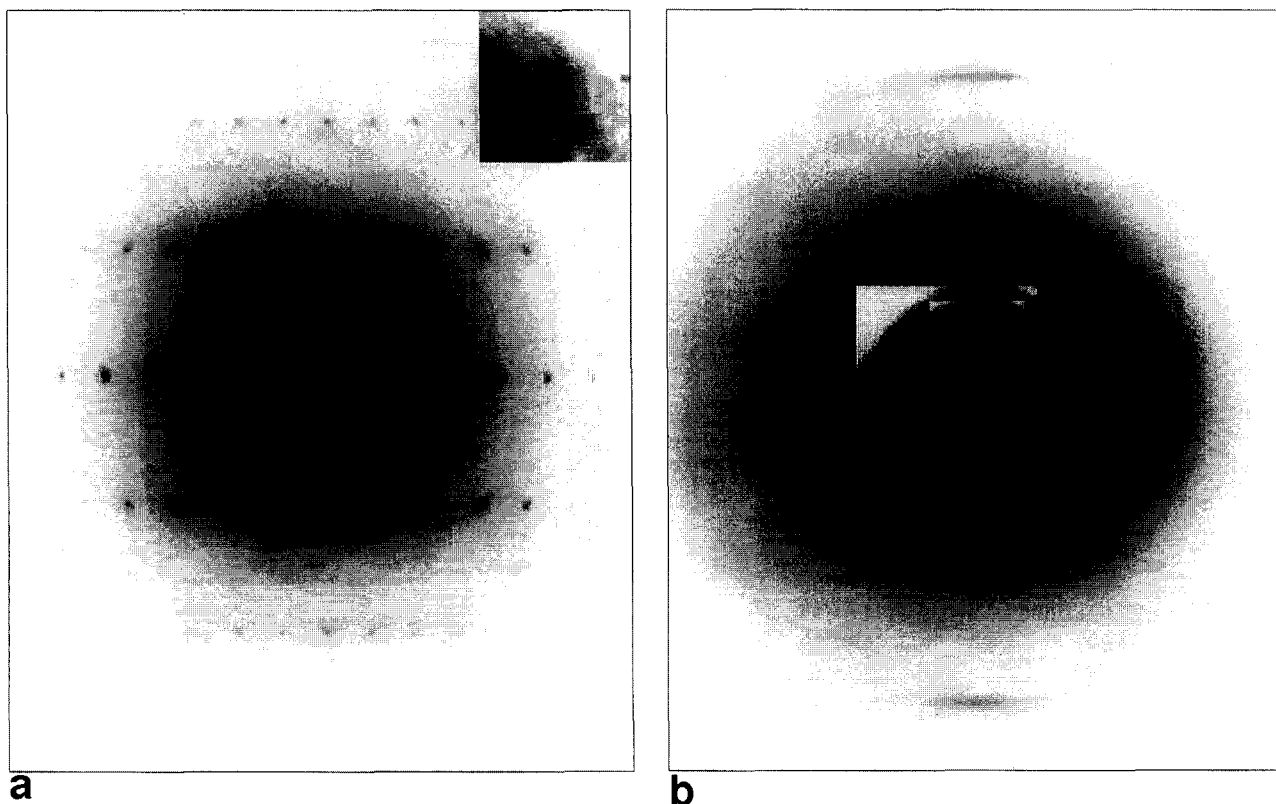


Figure 13 ED patterns of CTFMP-prepared PPONY (250°C, 4 h) (a) as polymerized and (b) after shearing at 320°C and annealing at 280°C for 7 h. The inset in (a) is an enlargement of the 510 reflection



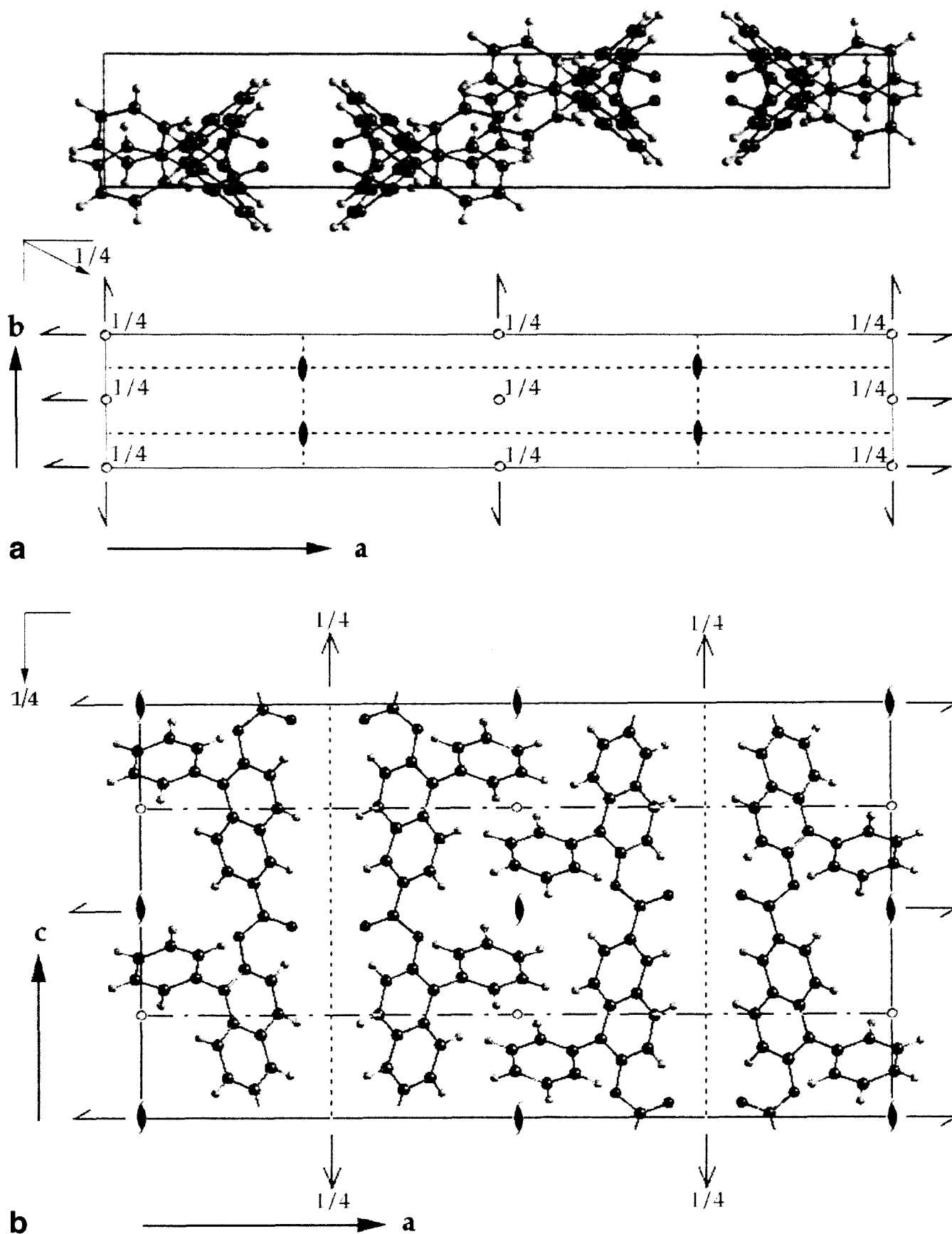


Figure 14 (a-c) Unit cell packing for PPNY as minimized by the Cerius<sup>2</sup> program for the  $P2_1/c2_1/c2/n$  space group. (d) Simulated [001] ED pattern corresponding to (a). (e) Simulated ED fibre pattern

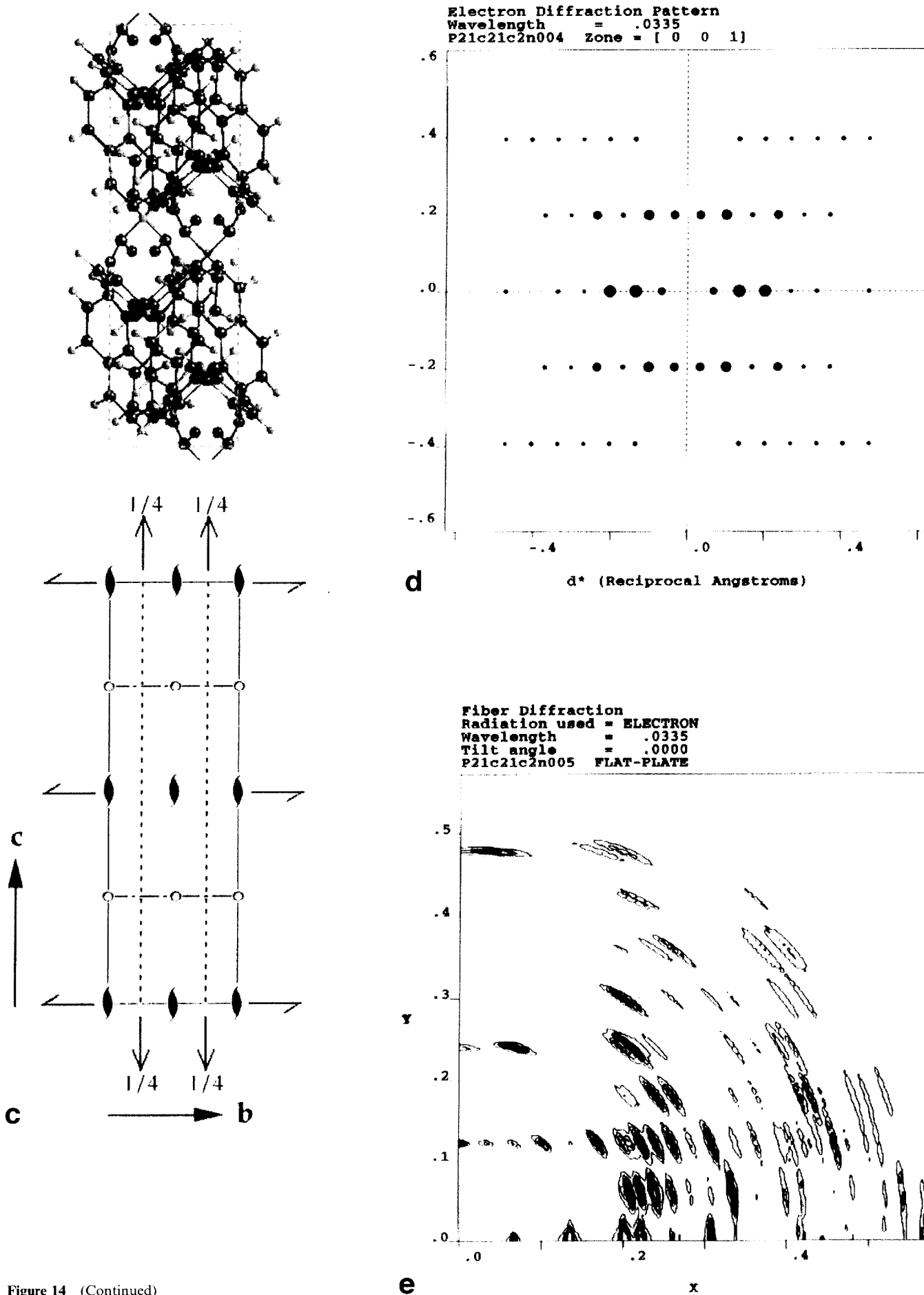


Figure 14 (Continued)

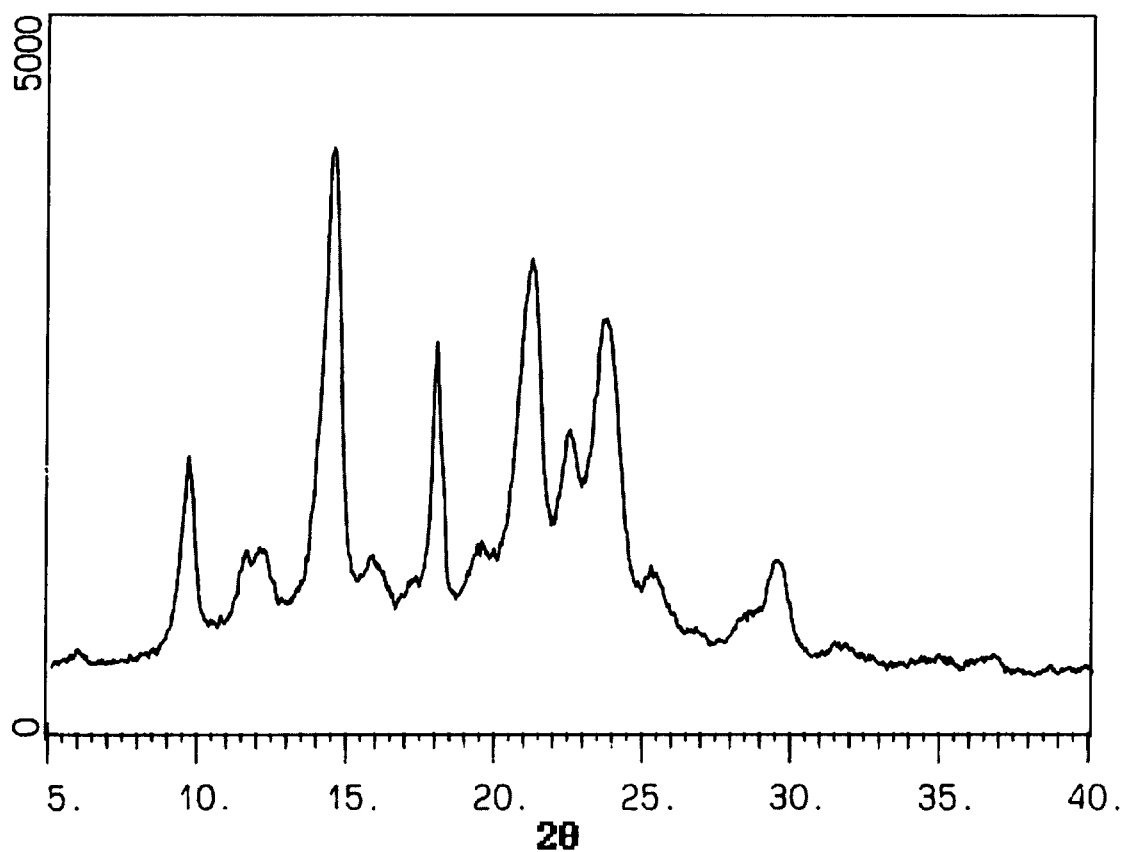


Figure 15 An X-ray diffraction scan from bulk-polymerized PPONY

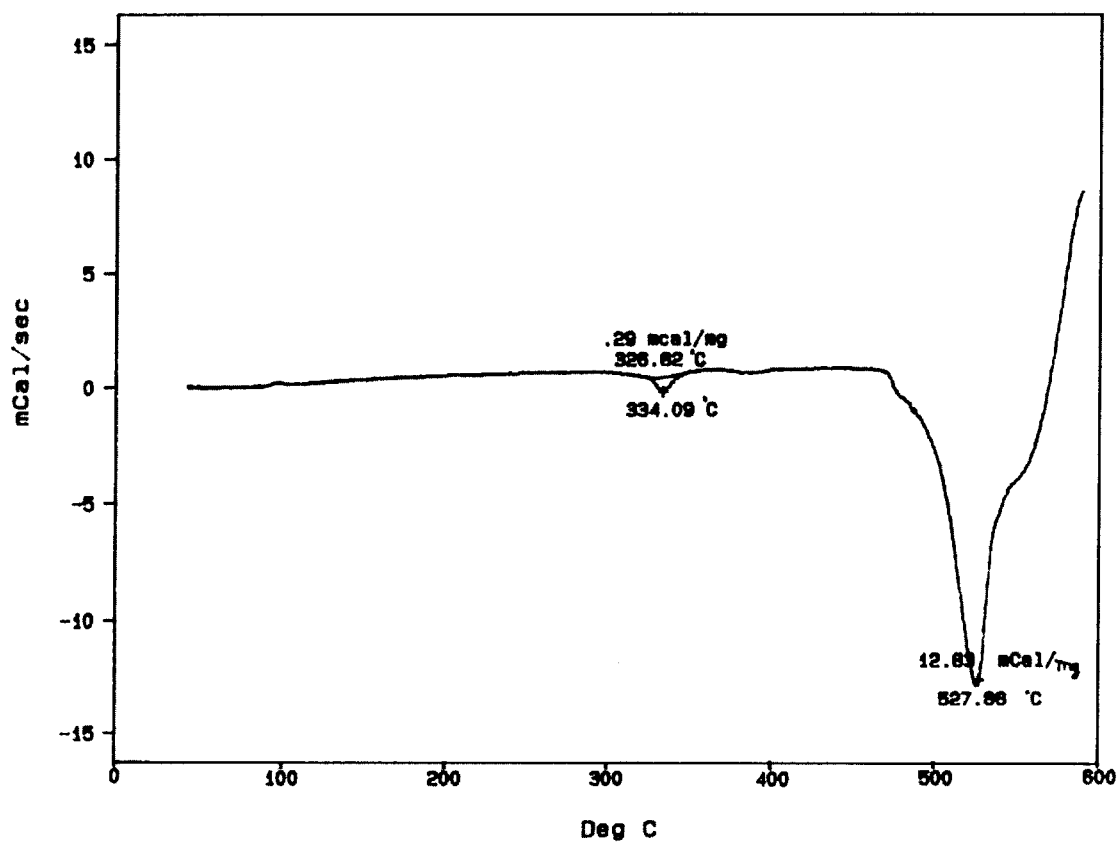


Figure 16 D.s.c. scan of bulk-polymerized PPONY

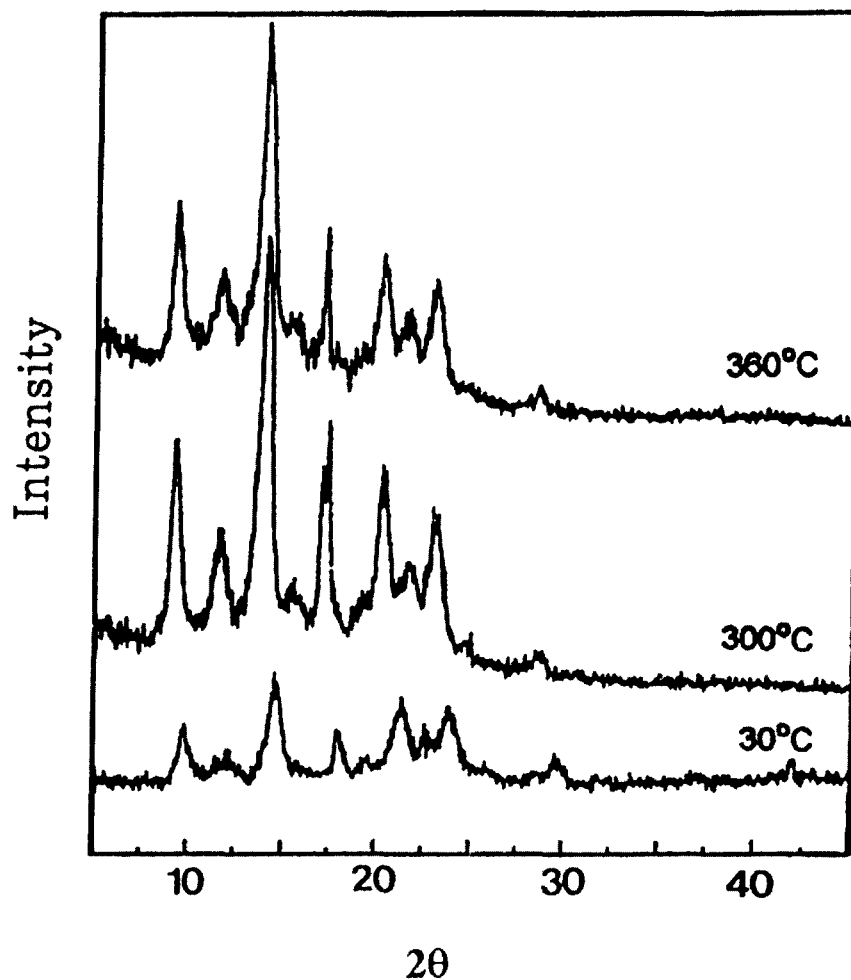


Figure 17 The X-ray scans of PPONY taken at room temperature, 300°C and 360°C

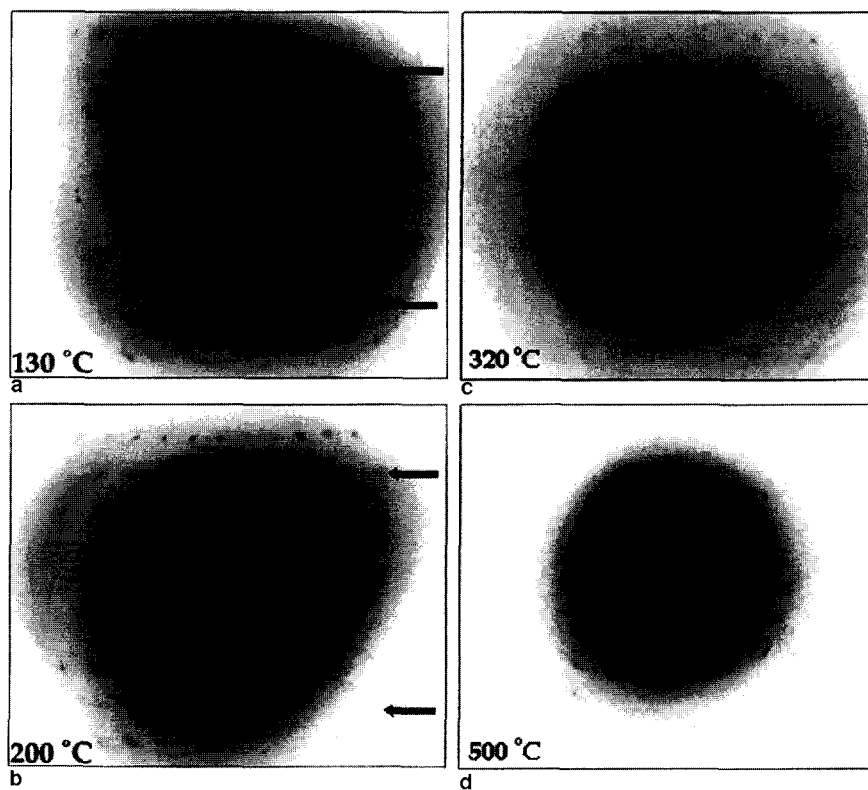
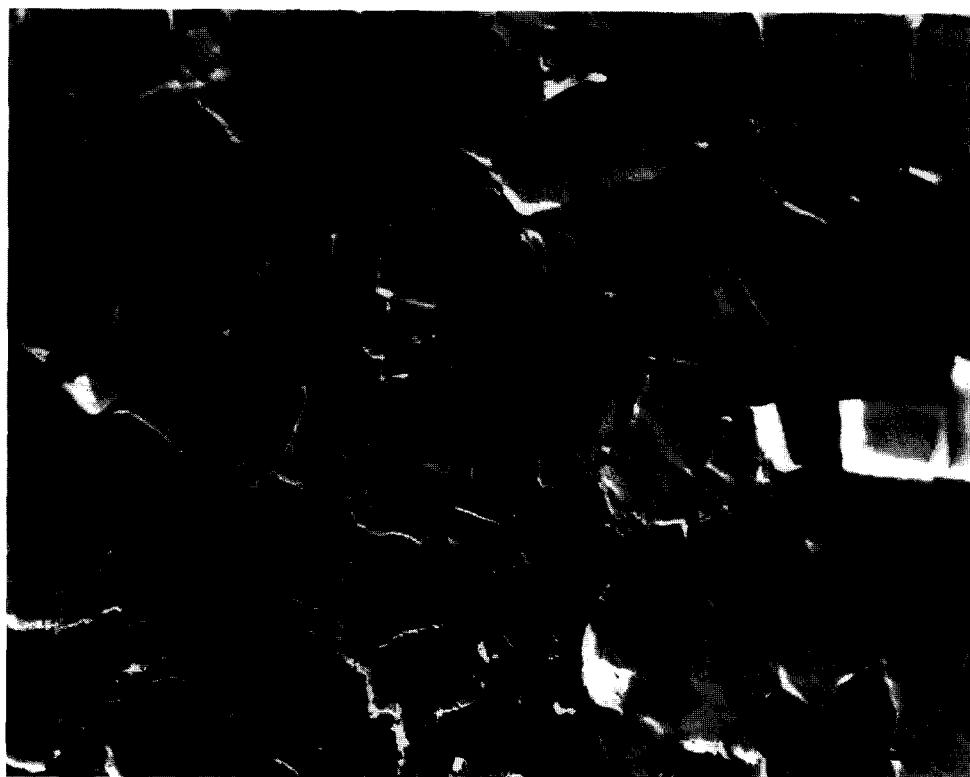


Figure 18 ED patterns of PPONY lath lamellae taken at (a) 130°C, (b) 200°C, (c) 320°C and (d) 500°C



**Figure 19** CTFMP-prepared PPONY heated to 550°C in the electron microscope hot stage and cooled to room temperature before shadowing. Fibres are indicated by arrows

#### ACKNOWLEDGEMENTS

This research was supported, in part, by grants from the National Science Foundation (DMR 93-12823) and the Korean Science and Engineering Foundation. A portion of this work was done while one of us (P.H.G.) was the Harold A. Morten Visiting Professor in the Department of Polymer Engineering at the University of Akron.

#### REFERENCES

- 1 Jackson, W. J. *Br. Polym. J.* 1980, **12**, 154
- 2 Rybnikar, F. and Geil, P. H. in 'Proceedings of the American Physical Society', Pittsburgh, PA, 1994
- 3 Economy, J., Storm, R. S., Matkovich, V. I., Cottis, S. G. and Novak, B. E. *J. Polym. Sci., Polym. Chem. Edn* 1976, **14**, 2207
- 4 Liu, J. and Geil, P. H. *Polymer* 1993, **34**, 1366
- 5 Cheng, S. Z. D., Johnson, R., Wu, Z. and Wu, H. H. *Macromolecules* 1991, **24**, 150
- 6 Huh, S. M., Jin, J. I., Liu, J., Long, T. C., Rybnikar, F. and Geil, P. H. in 'Proceedings of the Europhysics Macromolecules Conference', Prague, 1995
- 7 Antipov, E. M., Stamm, M., Abetz, V. and Fisher, E. W. *Acta Polym.* 1994, **45**, 196
- 8 Liu, J., Rybnikar, F., East, A. J. and Geil, P. H. *J. Polym. Sci., Polym. Phys. Edn* 1993, **31**, 1923
- 9 Liu, J., Rybnikar, F. and Geil, P. H. *J. Polym. Sci., Polym. Phys. Edn* 1992, **30**, 1969
- 10 Rybnikar, F., Liu, J. and Geil, P. H. *Macromol. Chem. Phys.* 1994, **195**, 81
- 11 Huh, S.-M. and Jin, J.-I. *Macromol. Symp.* in press
- 12 Kent, S. L. and Geil, P. H. *J. Polym. Sci., Polym. Phys. Edn* 1992, **30**, 1489
- 13 Rybnikar, F. and Geil, P. H. unpublished results
- 14 Schwarz, G. and Kricheldorf, M. R. *Macromolecules* 1994, **27**, 2395
- 15 Iannelli, P., Yoon, D. Y. Parrish, W. *Macromolecules* 1994, **27**, 3295